JOURNAL OF VIROLOGY, Mar. 2010, p. 2753–2761 Vol. 84, No. 6
0022-538X/10/$12.00 doi:10.1128/JVI.01813-09

Canine Distemper Viruses Expressing a Hemagglutinin without N-Glycans Lose Virulence but Retain Immunosuppression▽

Bevan Sawatsky and Veronika von Messling*

INRS-Institut Armand-Frappier, University of Quebec, Laval, Quebec, Canada

Received 27 August 2009/Accepted 18 December 2009

Paramyxovirus glycoproteins are posttranslationally modified by the addition of N-linked glycans, which are often necessary for correct folding, processing, and cell surface expression. To establish the contribution of N glycosylation to morbillivirus attachment (H) protein function and overall virulence, we first determined the use of the potential N-glycosylation sites in the canine distemper virus (CDV) H proteins. Biochemical characterization revealed that the three sites conserved in all strains were N glycosylated, whereas only two of the up to five additional sites present in wild-type strains are used. A wild-type virus with an H protein reproducing the vaccine strain N-glycosylation pattern remained lethal in ferrets but with a prolonged course of disease. In contrast, introduction of the vaccine H protein in the wild-type context resulted in complete attenuation. To further characterize the role of N glycosylation in CDV pathogenesis, the N-glycosylation sites of wild-type H proteins were successively deleted, including a nonstandard site, to ultimately generate a nonglycosylated H protein. Despite reduced expression levels, this protein remained fully functional. Recombinant viruses expressing N-glycan-deficient H proteins no longer caused disease, even though their immunosuppressive capacities were retained, indicating that reduced N glycosylation contributes to attenuation without affecting immunosuppression.

Measles virus (MeV) and *Canine distemper virus* (CDV) are members of the genus *Morbillivirus* in the family *Paramyxoviridae* that are highly contagious and can cause severe disease. MeV is known to infect only humans and certain nonhuman primates and is rarely fatal, while CDV infects a broad range of carnivores and can result in up to 100% mortality (13). The signaling lymphocyte activation molecule (SLAM; CD150), which is expressed on activated T and B cells (10), is the primary receptor for morbilliviruses (3, 15, 42). Morbillivirus attachment to susceptible cells occurs via interaction between SLAM and the viral hemagglutinin (H) protein, one of two glycoproteins that are inserted into the viral membrane and subsequently expressed on the surfaces of infected cells. Upon binding, the conformational change of the H protein conducts a signal to the fusion (F) protein, which then mediates fusion between the viral and host cell membranes. However, the extent and efficiency of cell-cell fusion are H protein dependent (21, 52).

Morbillivirus vaccine strains were developed during the 1960s by serial passages in eggs and different cell lines (11, 35). Consequently, there are significant molecular differences between the glycoproteins of wild-type and vaccine CDV strains. The H protein of the large-plaque Onderstepoort strain (OL) differs from the wild-type 5804P at 60 amino acid residues, introducing several additional N-glycosylation sites. Based on the observation that the vaccine strain H proteins have a lower apparent molecular weight than the wild-type proteins (9, 52), it has been hypothesized that reduced N glycosylation is an important attenuating factor and that an increase in N glycosylation may eventually result in vaccine failure (19).

Posttranslational modifications, including N-linked glycosylation, are essential for the functions of many integral membrane and secreted proteins. N-glycan chains are added to asparagine (N) residues in the endoplasmic reticulum (ER) at the consensus sequence N-X-S/T, where "X" can be any amino acid except proline. As the nascent protein chain is inserted into the ER and moves through the Golgi apparatus and finally to the plasma membrane, N-glycans are trimmed and modified into elaborate structures that can account for a substantial proportion of the overall molecular weight of a given glycoprotein (43). N glycosylation has been shown to be important for the correct folding, transport, and function of other paramyxovirus fusion and attachment glycoproteins, including MeV H (17), Sendai virus hemagglutinin-neuraminidase (HN) (39), simian virus 5 HN (31), and Newcastle disease virus HN (27). In most cases, one or two N-glycans at specific locations are essential for proper folding and transport to the cell surface, and at least one or two N-glycans are required for the F or H/HN protein to function correctly (30, 47). Thus, the total deletion of N-glycans is generally not tolerated.

To characterize the contribution of H protein N glycosylation to morbillivirus pathogenesis, we took advantage of the CDV ferret model (48, 50). We first determined the role of decreased natural N glycosylation of the vaccine strain H protein in protein function and virulence. Based on our finding that reduced N glycosylation results in prolonged disease, we performed a comprehensive mutational analysis to determine the minimal complement of H protein N glycosylation needed for proper intracellular transport and function. Using viruses bearing increasingly deglycosylated H proteins, we demonstrate that a CDV H protein without N-glycans remains completely functional. However, minimal N glycosylation is required for virulence.

* Corresponding author. Mailing address: INRS-Institut Armand-Frappier, University of Quebec, 531 boulevard des Prairies, Laval, Québec, H7V 1B7, Canada. Phone: (450) 687-5010, ext. 8872. Fax: (450) 686-5501. E-mail: veronika.vonmessling@iaf.inrs.ca.

▽ Published ahead of print on 30 December 2009.

MATERIALS AND METHODS

Cells and transfections. Vero cells stably expressing canine SLAM (Vero dogSLAMtag) (50) and 293 cells (ATCC CRL-1573) were maintained in Dulbecco's modified Eagle medium (DMEM) (Gibco) supplemented with 5% heat-inactivated fetal bovine serum (FBS). For the biochemical analysis of recombinant proteins, 12-well plates of Vero dogSLAMtag cells were transfected at approximately 90% confluence as described previously (37). Briefly, each well was transfected with 2 μg of the H expression plasmid pCG-H5804Pzeo or the respective mutant H plasmids using Lipofectamine 2000 (Invitrogen). Fusion activity was evaluated after 24 h. To harvest protein lysates, 200 μl of RIPA buffer (50 mM Tris-HCl, pH 8.0, 150 mM NaCl, 1% NP-40, and 0.5% sodium deoxycholate) containing protease inhibitor cocktail (Complete; Roche) was added to the transfected cells 16 h after transfection. The lysate was collected and centrifuged at 14,000 × *g* for 15 min at 4°C, and the clarified lysate was stored at −20°C.

Production of recombinant CDV H proteins. To generate mutant H proteins, the 5804P H gene was subcloned into pCR4-TOPO to yield CDV H-TOPO. The initial round of N-glycosylation mutations (N149Q, N309Q, N391Q, N422Q, N456Q, N587Q, and N603Q) was performed on CDV H-TOPO, and the mutant genes were subcloned into pCG-IREShygromut (50) using the BamHI and SphI restriction sites. These plasmids were used for all subsequent mutageneses. To generate mutant H proteins with vaccine-like N-glycosylation patterns and C-terminal truncations, S605 was first changed to a stop codon (S605stop), after which the mutations N309Q, N391Q, and N456Q were introduced into this clone, yielding pCG-$H_{OL\text{-}like}$.

To generate the corresponding recombinant viruses, the respective mutated fragments were subcloned into a genomic segment containing the 5804P H open reading frame (ORF) and then transferred into the full-length p5804PeH plasmid, which expresses enhanced green fluorescent protein (EGFP) from an additional open reading frame located between the H and polymerase genes (48), using the BsrGI and AscI sites, yielding p5804P-H_{OL}, p5804P-$H_{OL\text{-}like}$, p5804P-H_{5ko}, and p5804P-H_{6ko}. The sequences of all clones were verified.

Recovery and amplification of recombinant viruses. Recombinant viruses were recovered as previously described (1, 24). Briefly, semiconfluent 293 cells were transfected with 6 μg of the respective CDV genomic plasmid and a combination of 0.5, 0.1, 0.5, and 0.7 μg MeV N, P, polymerase (L), and T7 RNA polymerase expression plasmid, respectively, using TransIT-LT1 (Mirus). Three days post-transfection, the cells were resuspended and overlaid onto Vero dogSLAMtag cells at 80 to 90% confluence in 10-cm dishes. The cocultured cells were maintained in DMEM containing 5% FBS until syncytia were observed. Individual syncytia were then picked and inoculated onto fresh Vero dogSLAMtag cells. Stocks of the recombinant viruses and the parental recombinant 5804PeH strain were grown on Vero dogSLAMtag cells. Titrations were performed by limiting dilution of virus stock in DMEM containing 5% FBS and expressed as the 50% tissue culture infectious dose ($TCID_{50}$). For growth kinetics, cells were infected at a multiplicity of infection (MOI) of 0.01 for each recombinant virus, and supernatant and cell-associated virus titers were followed for 5 days.

Western blots and cell surface biotinylation. For each protein, 10 μl of RIPA lysate was mixed with 10 μl of 2× SDS–gel-loading buffer (SDS-GLB) containing 40% β-mercaptoethanol. Protein lysates were separated by SDS-PAGE on 4% stacking/8% resolving gels, transferred to polyvinylidene difluoride (PVDF) membranes, and blocked overnight at 4°C in 0.5% blocking reagent (Roche) prepared in Tris-buffered saline (TBS). The blocked membranes were probed with the Hcyt antiserum, which recognizes the cytoplasmic tail of CDV H (52), followed by detection with goat anti-rabbit horseradish peroxidase (HRP)-conjugated secondary antibody (Sigma) using the ECL^+ Chemiluminescence detection kit (GE Healthcare).

Cell surface biotinylation was performed as described previously (47). Transfected cell monolayers were biotinylated for 20 min at 4°C with EZ-Link Sulfo-NHS-LC-biotin (Pierce) at a concentration of 2 mM in 750 μl/well of ice-cold PBS and then washed with ice-cold PBS plus 100 mM glycine to quench excess biotin. The cells were lysed in 600 μl/well of RIPA buffer with protease inhibitor, a 20-μl aliquot was taken for Western blot analysis, and 1 μl/tube of Hcyt antiserum and 60 μl/tube of immobilized protein A beads (Thermo Scientific) were added to the clarified RIPA lysate. After incubation overnight at 4°C on a rotating tube rack, the beads were washed three times with RIPA buffer and mixed with 30 μl of 1× SDS-GLB and heated at 75°C for 5 min. The crude lysates and immunoprecipitated proteins were separated in parallel on SDS-PAGE gels and transferred to PVDF membranes. Total cellular expression of recombinant H proteins was detected as described above, while biotinylated proteins were detected using a streptavidin-HRP conjugate (Pierce) and the ECL^+ Chemiluminescence kit (GE Healthcare). Bands were quantified using Molecular Imaging software (Kodak).

***In vivo* characterization of recombinant viruses.** Unvaccinated male ferrets (*Mustela putoris furo*) aged 16 weeks and older (Marshall Farms) were used for all studies. All animal experiments were performed as described previously (48, 50) and were approved by the institutional animal care and use committee of the INRS-Institut Armand-Frappier. Groups of three to six ferrets were infected intranasally with 10^5 $TCID_{50}$ of the respective virus. Body temperature and clinical signs were recorded daily, and blood samples were collected from the jugular vein under general anesthesia twice weekly for the first 2 weeks and weekly thereafter. Clinical signs, such as the development of rash or fever, were monitored daily. Four parameters of virulence were measured. Rash was graded 0 (no rash), 1 (localized rash), or 2 (generalized rash); fever was graded 0 (no fever), 1 (temperature reached above 39°C), or 2 (temperature reached above 40°C); and weight loss was classified as 0 (0 to 5% loss of day 0 body weight), 1 (5 to 10% loss of day 0 body weight), or 2 (more than 10% loss of day 0 body weight). Cell-associated viremia was determined by limiting dilution of peripheral blood mononuclear cells (PBMCs) as described previously (6, 51). *In vitro* proliferation of Ficoll-purified PBMCs was assessed by stimulation with 1 μg/ml phytohemagglutinin (PHA) and subsequent detection of bromodeoxyuridine (BrdU) incorporation into proliferating cells using the Cell Proliferation ELISA BrdU kit (Roche).

Neutralizing-antibody titers were determined by mixing serial dilutions of plasma collected at different time points with 10^2 $TCID_{50}$ of 5804PeH. For cross-neutralization experiments, 10^2 $TCID_{50}$ of either 5804P-H_{6ko} or 5804P-H_{OL} was used, in addition to 5804PeH. Control plasma samples for 5804P-positive ferrets were taken from a group of animals that had been vaccinated using the envelope proteins of 5804P and that were then challenged with 5804PeH (36). The virus and plasma were incubated at 37°C for 15 min before 50 μl of Vero dogSLAMtag cells was added to each well. The neutralizing titer was expressed as the reciprocal of the highest dilution at which no cytopathic effect (CPE) was observed after 4 days.

RESULTS

A wild-type H protein with a vaccine-like glycosylation pattern is fully functional. The vaccine strain OL H protein (H_{OL}) has three fewer potential N-linked glycosylation sites than the 5804P H protein (H_{5804P}) due to the following changes in the amino acid sequence: N309S, T393A, and N456D. In addition, a mutation at S605 results in a premature stop codon, truncating the H_{OL} ORF by 3 amino acids. This truncation also disrupts the N-glycosylation sequon at residues 603 to 605, thereby eliminating the potential N-glycosylation site, leaving H_{OL} with three potential N-glycosylation sites (Fig. 1A). To determine if lack of these N-glycosylation sites accounts for the observed differences in the apparent molecular weights of vaccine and wild-type H proteins (9, 52), we mutated the wild-type protein to correspond to H_{OL} in length and N-glycosylation pattern, which we named $H_{OL\text{-}like}$ (Fig. 1A). $H_{OL\text{-}like}$ and the parental proteins were expressed at similar levels, and H_{OL} and $H_{OL\text{-}like}$ migrated faster than H_{5804P} (Fig. 1B). Treatment with PNGase F, which removes all N-linked glycans, resulted in similar migration patterns for all proteins, indicating that the observed differences are largely due to N-linked glycosylation. Surface biotinylation revealed that $H_{OL\text{-}like}$ is transported to the cell surface less efficiently than H_{5804P} or H_{OL} (Fig. 1C). However, its fusion activity upon cotransfection with the F protein in Vero dogSLAMtag cells was similar to that of the parental proteins (Fig. 1D), demonstrating that $H_{OL\text{-}like}$ is functional. The identity of the higher-molecular-weight band in Fig. 1C is unknown, but it likely represents a protein that coimmunoprecipitates with H, since it is not present in mock-transfected cells.

Introduction of either the H_{OL} or the $H_{OL\text{-}like}$ protein into the 5804P background resulted in recombinant viruses that

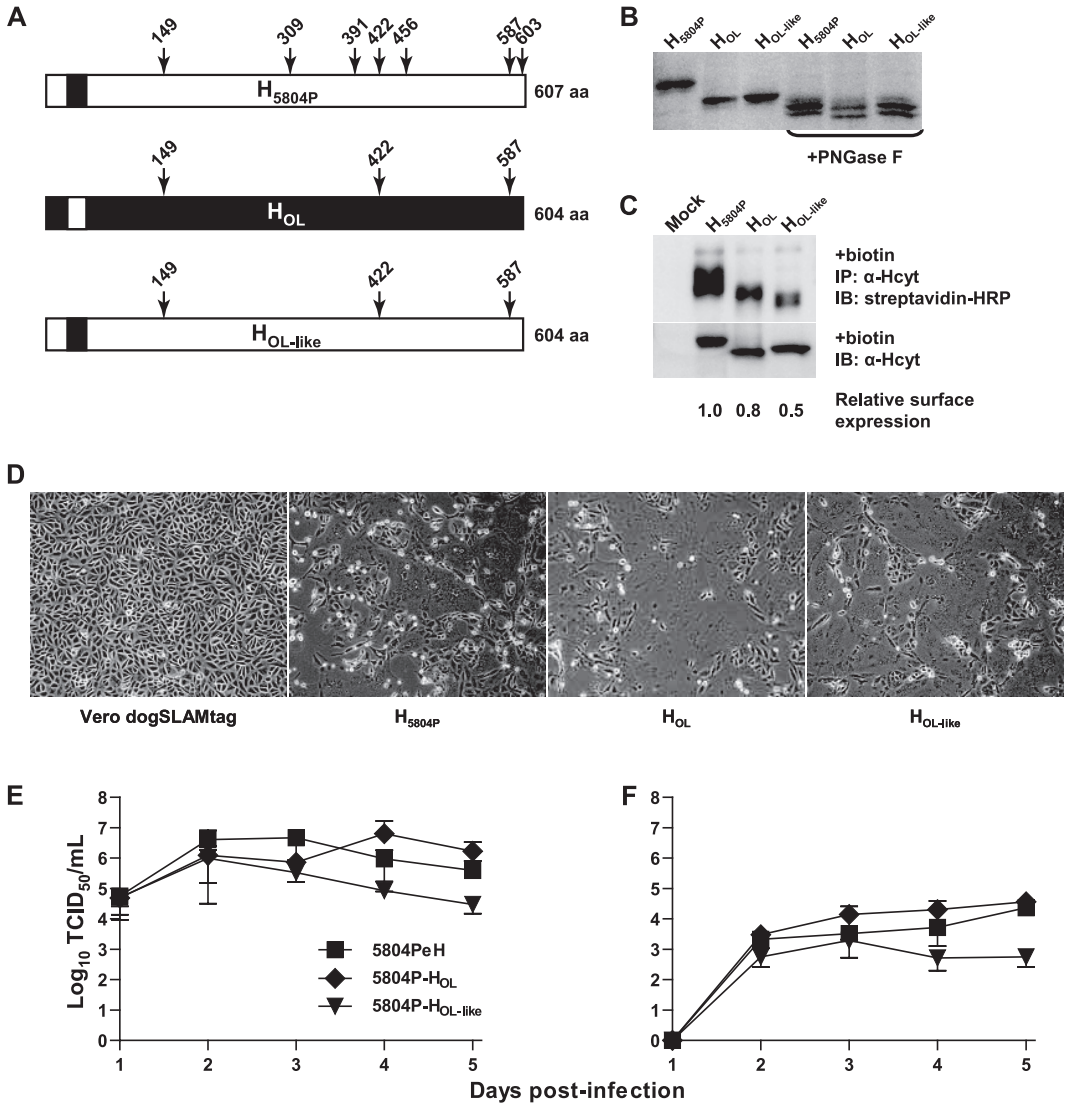

FIG. 1. Construction and characterization of recombinant viruses with vaccine-like H protein N glycosylation. (A) Schematic drawing of the H_{5804P} and H_{OL} proteins. The $H_{OL\text{-}like}$ protein has the primary sequence of H_{5804P} with the mutations N309Q, N391Q, N456Q, and S605stop to reproduce the glycosylation pattern of H_{OL}. Protein schematics are shown from the N to the C terminus. The N-terminal box represents the cytoplasmic tail, the black box represents the transmembrane domain, and the C-terminal box represents the C-terminal ectodomain. (B) Western blot analysis of vaccine-like H protein expression. H_{5804P}, H_{OL}, and $H_{OL\text{-}like}$ were expressed in Vero dogSLAMtag cells by transfection of expression plasmids and detected by Western blotting. Each lysate was also treated with PNGase F to remove all N-glycans. (C) Cell surface biotinylation of vaccine-like H proteins. Cells transfected with expression plasmids for H_{5804P}, H_{OL}, or $H_{OL\text{-}like}$ were labeled with Sulfo-NHS-LC-biotin, immunoprecipitated (IP) with an antiserum recognizing the H protein cytoplasmic tail, and detected with a streptavidin-HRP conjugate. Western blots of cell lysates from the same experiment were analyzed for total H protein expression. The relative surface expression of each protein was calculated by normalizing the biotinylation or Western blot signal to the respective H_{5804P} signal. The relative surface expression represents the ratio between the normalized biotinylation signal and the normalized Western blot signal for each replicate. Average relative surface expression is shown, and the blots are representative of three independent replicates. IB, immunoblot. (D) Cell-cell fusion observed for wild-type and mutant H proteins. Confluent monolayers of Vero dogSLAMtag cells were transfected with F_{5804P} in combination with H_{5804P}, H_{OL}, or $H_{OL\text{-}like}$ expression plasmid. The images were taken 24 h posttransfection at ×100 magnification. The left image shows control untransfected Vero dogSLAMtag cells. (E and F) Growth kinetics of recombinant 5804P viruses expressing either H_{5804P}, H_{OL}, or $H_{OL\text{-}like}$ in Vero dogSLAMtag cells shown as either cell-associated (E) or released (F) virus. The cells were infected at an MOI of 0.01, and samples were harvested daily for 5 days. Titers are expressed as $TCID_{50}$/ml, and the error bars indicate standard deviations.

replicated efficiently and showed similar growth kinetics with respect to cell-associated (Fig. 1E) and supernatant (Fig. 1F) titers.

H protein glycosylation contributes to virulence. To assess the impact of the reduction in N-glycans on pathogenesis, ferrets were infected intranasally with 10^5 $TCID_{50}$ of the respective recombinant virus. Animals infected with 5804PeH developed a severe rash with fever and weight loss, succumbing to disease 12 to 13 days after infection (Fig. 2A and B). In contrast, 5804P-H_{OL}-infected ferrets showed no clinical signs, although two animals lost a small amount of weight, and all survived (Fig. 2A and B). Infection with 5804P-$H_{OL\text{-}like}$ re-

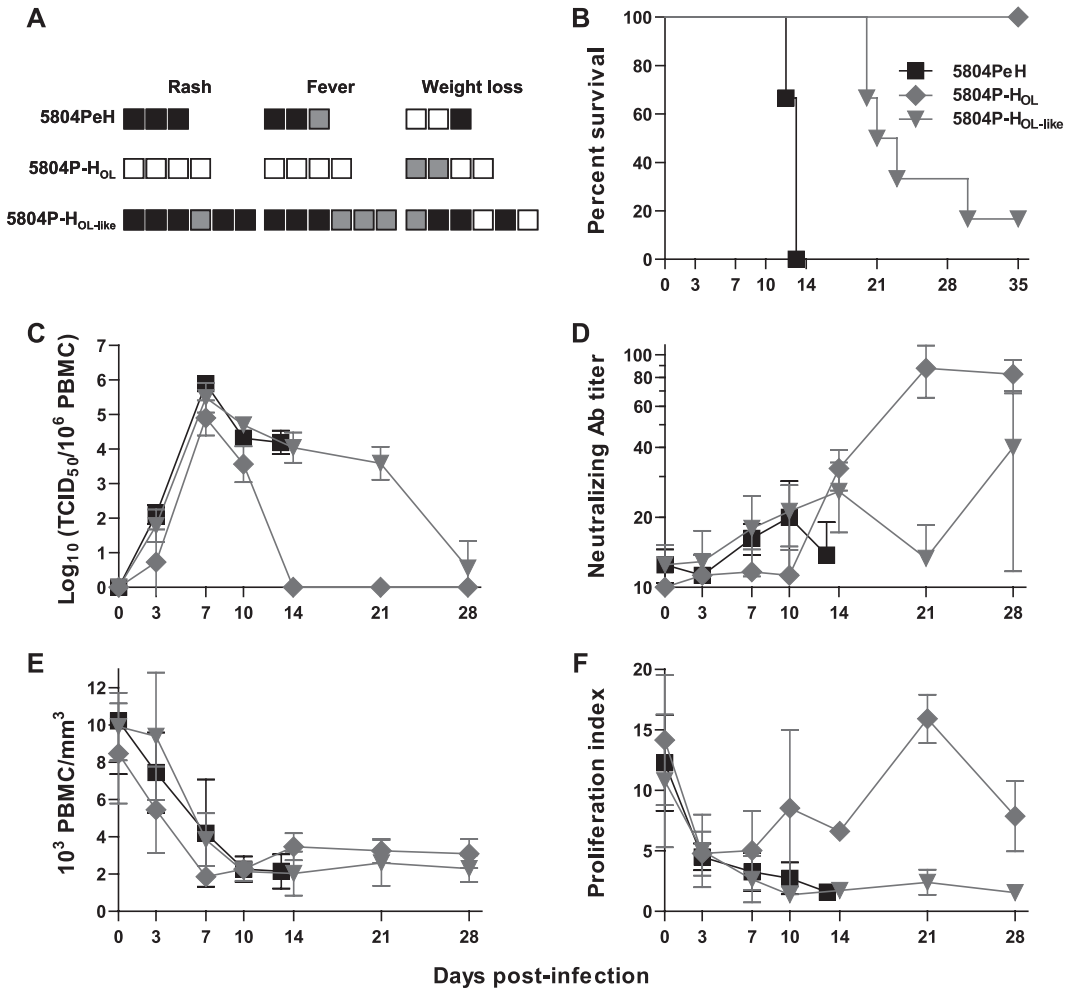

FIG. 2. Virulence of vaccine-like viruses in ferrets. Groups of three to six animals were infected intranasally with 10^5 $TCID_{50}$ of either the recombinant parental 5804PeH virus or the recombinant viruses 5804P-H_{OL} and 5804P-$H_{OL\text{-}like}$. (A) Virulence index. Each box represents one animal, and black represents the highest (2), gray an intermediate (1), and white the lowest (0) score, as detailed in Materials and Methods. (B) Survival curve. Death of an animal is indicated by a step down on the curve. (C) The course of cell-associated viremia is shown as the $\log_{10}$ of the virus titer per 10^6 PBMCs. (D) CDV neutralizing-antibody response in plasma samples. Antibody titers are shown as reciprocals of the highest dilution in which CPE was observed. (E) Total leukocyte counts from infected animals, shown as 10^3 leukocytes per mm^3. (F) *In vitro* proliferation activities of lymphocytes from infected animals. Days postinfection are indicated on the *x* axes of the graphs, and the error bars represent standard deviations.

sulted in an intermediate disease phenotype, characterized by substantial rash and fever and delayed mortality. Two animals were found to have severe bacterial pneumonia at the time of sacrifice, and one of the six animals survived (Fig. 2A and B). All animals became viremic with peak titers after 7 days, although the titer of 5804P-H_{OL} was approximately 5- to 10-fold lower than those of the other two viruses (Fig. 2C). The viral loads in the 5804PeH and 5804P-$H_{OL\text{-}like}$ groups remained high until the animals were sacrificed, with the exception of the survivor in the 5804P-$H_{OL\text{-}like}$ group, which remained viremic until day 28, while ferrets infected with 5804P-H_{OL} cleared the virus after 14 days (Fig. 2C). As previously reported for lethal infections (50), 5804PeH or 5804P-$H_{OL\text{-}like}$ generally elicited a very poor neutralizing-antibody response, while infection with 5804P-H_{OL} resulted in titers within the protective range by day 35 (Fig. 2D). Both 5804PeH and 5804P-$H_{OL\text{-}like}$, which were lethal, caused severe immunosuppression, as indicated by dramatically decreased white blood cell counts (Fig. 2E) and severe inhibition of PBMC proliferation (Fig. 2F), whereas animals infected with 5804P-H_{OL} experienced only a transient decrease in proliferation (Fig. 2F) despite severe leukopenia (Fig. 2E).

A completely deglycosylated CDV H retains function. To characterize H protein N glycosylation in more detail, we produced a comprehensive panel of further H_{5804P} N-glycan deletion mutants. The H_{5804P} protein has seven potential N-glycosylation sites of the type N-X-S/T at positions N149, N309, N391, N422, N456, N587, and N603 of its ectodomain (Fig. 3A), and one additional site has been reported at position 584 of some Asian isolates (19, 29). Only disruption of N-glycosylation sequons at the sites N149, N391, N422, N456, and N587 resulted in mutant proteins that migrated at a slightly variable but uniformly lower apparent molecular weights than the parental H_{5804P} protein, while those with the mutations

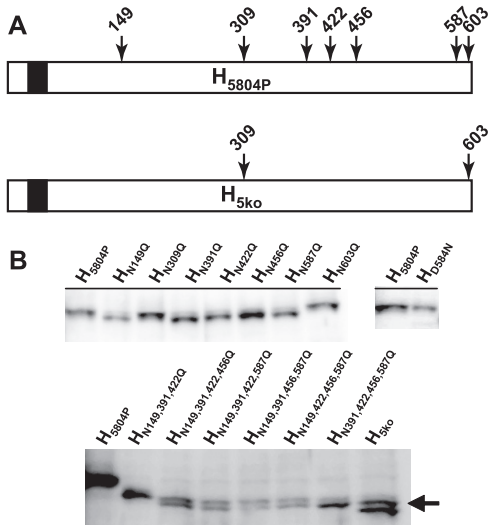

FIG. 3. Systematic deglycosylation of H_{5804P}. (A) Schematic drawing of the N-glycosylation sites of the type N-X-S/T located in the ectodomain of H_{5804P} and the mutant protein H_{5ko}. Protein schematics are shown from the N terminus (left) to the C terminus (right). The N-terminal white boxes represent the cytoplasmic tail, the black boxes the transmembrane domain, and the C-terminal white boxes the ectodomain. (B) Western blot expression analysis of a comprehensive panel of N-glycosylation knockout mutant H_{5804P} proteins. Proteins were expressed by transfection of expression plasmids in Vero dogSLAMtag cells. (Top) Single N-glycan knockout proteins (left blot) and the H_{D584N} knock-in mutant protein (right blot) compared to H_{5804P} protein. Note that H_{N309Q}, H_{N603Q}, and H_{D584N} do not shift in apparent molecular weight. (Bottom) Quadruple- and quintuple-knockout proteins produced in all possible combinations. Mutant proteins are shown with H_{5804P} and $H_{N149,391,422Q}$ to illustrate the observed molecular weight shift. The arrow indicates the higher-molecular-weight band observed for H_{5ko}.

N309Q and N603Q, as well as D584N, which introduces the site found in some Asian isolates, retained the parental molecular weight (Fig. 3B). Based on the five N-glycosylation sites that were used, a full panel of mutants was constructed lacking two, three, four, or five N-glycans in all possible combinations (Fig. 3B). All of these recombinant proteins remained functional in a cell-cell fusion assay (data not shown).

Curiously, a distinct double band that comigrated with a glycoform having an additional N-glycan was observed in proteins lacking four or more N-glycans (Fig. 3B). This higher-molecular-weight band was sensitive to treatment with PNGase F (data not shown), indicating that it is due to one or more extra N-glycans. While H_{5ko} lacks all five N-glycosylation sites used in H_{5804P}, it still contains the sites at N309 and N603 (Fig. 4A), which were not used in the wild-type context. However, H_{7ko}, which carries the corresponding mutations, retained the double band (Fig. 4B and data not shown), demonstrating that alternative N glycosylation at these sites is not responsible for the larger band. In addition to these seven previously mentioned sites, there is a potential N-glycosylation site at residues 19 to 21 (NSS) in the cytoplasmic tail, which is unlikely to be used, and an N-X-C sequon at residues 152 to 154 (NYC) in the ectodomain (Fig. 4A). N glycosylation at N-X-C sites is uncommon but was first discovered in synthetic peptides, where the motif could act as an N-glycan acceptor (5), and was subsequently identified in several viral and cellular glycoproteins (28, 32, 41, 44, 45). Using H_{7ko}, we generated additional mutant proteins lacking N19 and N152 alone or in combination (H_{9ko}), ultimately resulting in complete removal of all potential N-glycosylation sites (Fig. 4A). As expected, mutation of N19 had no effect on the higher-molecular-weight band, but removal of N152 resulted in the band's disappearance (Fig. 4B), confirming that the nonstandard N-glycosylation site at N152 can be used in H_{5804P}. We then introduced the N152Q mutation into H_{5ko} to generate H_{6ko} (Fig. 4A), which comigrated with H_{9ko} as a single band, yielding a completely deglycosylated H protein with minimal amino acid changes (Fig. 4B). The total protein expression levels of all mutant H proteins were at least 2- to 3-fold reduced compared to H_{5804P} (Fig. 4B and C, bottom). However, the relative cell surface expression levels of H_{5ko} and its derivatives were similar to those of the wild-type H protein, while H_{6ko} surface expression was slightly lower (Fig. 4C, top). All mutant H proteins supported cell-cell fusion at wild-type levels (Fig. 4D), and the fusion associated with H_{7ko} was even slightly increased, which correlates with its higher relative cell surface expression (Fig. 4C and D).

To assess the functionality of these mutants in the viral context, recombinant 5804PeH viruses expressing the H_{5ko} and H_{6ko} proteins were recovered. The viruses with N-glycan-deficient H proteins grew to overall titers comparable to those of 5804PeH (Fig. 4E) but were slightly deficient in virus release, with titers becoming detectable only at 3 days postinfection for 5804P-H_{6ko} (Fig. 4F).

CDV H N glycosylation is essential for disease progression. To determine the importance of H protein N glycosylation for virulence, three ferrets were infected intranasally with 10^5 $TCID_{50}$ of 5804P-H_{5ko} or 5804P-H_{6ko}. None of the animals developed signs of disease except slight weight loss (Fig. 5A), and no mortality was observed. Even though the peak viral loads in PBMCs associated with 5804P-H_{5ko} and 5804P-H_{6ko} were similar to that of 5804PeH, the animals rapidly controlled the infection, resulting in complete clearance within 21 days (Fig. 5B). Animals infected with 5804P-H_{5ko} or 5804P-H_{6ko} developed strong leukopenia and inhibition of lymphocyte proliferation comparable to levels seen in 5804PeH-infected animals at days 10 to 14 after infection, which persisted for up to 35 days (Fig. 5C and D). All animals infected with N-glycan-deficient viruses mounted a neutralizing antibody response, but the levels remained slightly below the value considered sufficient for protection against subsequent infection (Fig. 5E). To evaluate the possibility that increased N glycosylation reduced the neutralization by sera raised against less glycosylated viruses, we tested the neutralization of 5804PeH, 5804P-H_{OL}, and 5804P-H_{6ko} by homologous and heterologous antisera. There was no difference in neutralization of 5804PeH or 5804P-H_{6ko} by antisera raised against either virus (Fig. 5F). Neutralization of 5804P-H_{OL} by its homologous antiserum was significantly stronger than neutralization by the anti-5804P and anti-5804P-H_{6ko} sera, which was, however, similar to neutralization levels observed for the other two viruses (Fig. 5F).

DISCUSSION

Most glycoproteins require a minimal level of N glycosylation to be functional. Paramyxovirus attachment proteins have at least

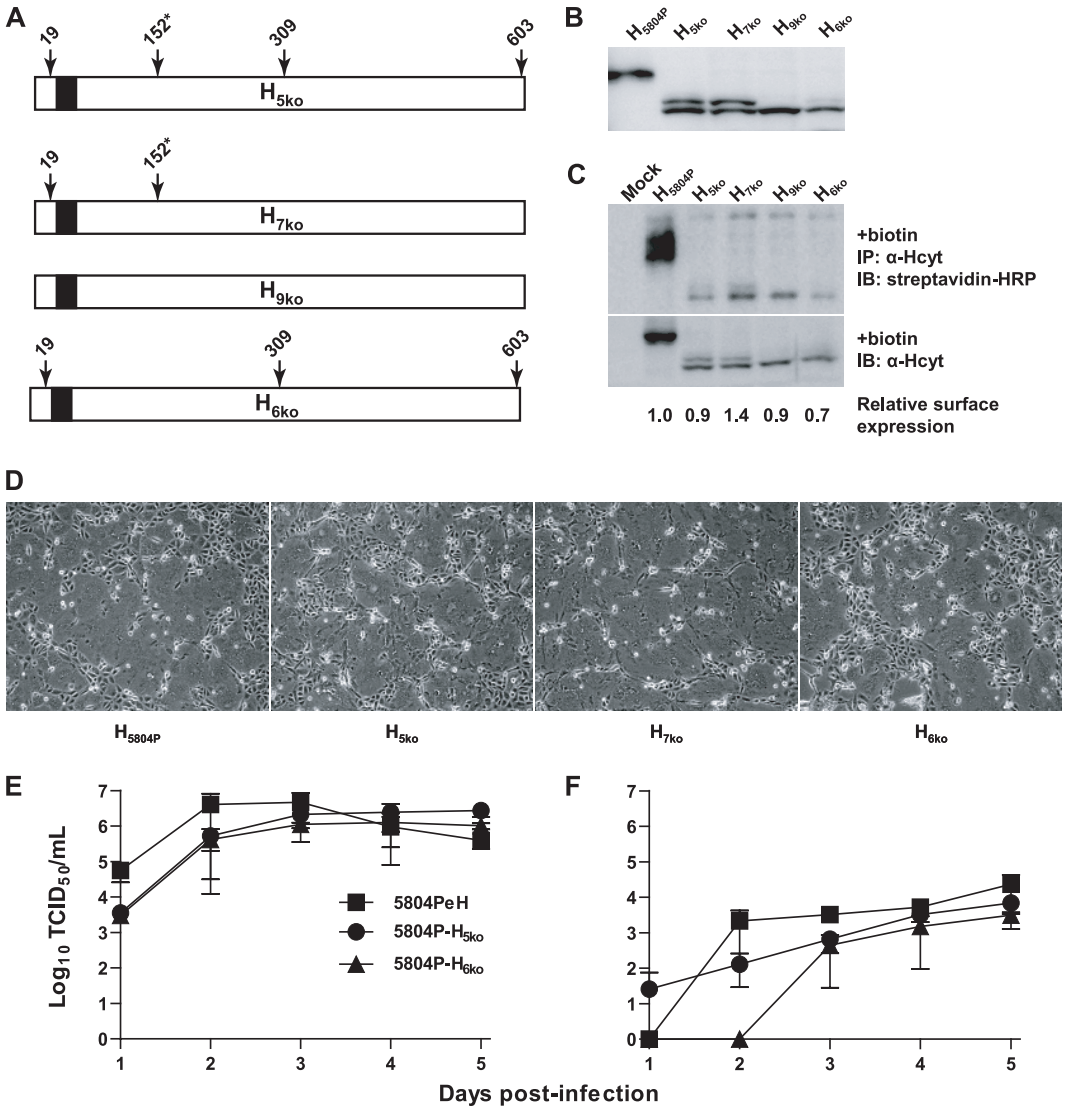

FIG. 4. Identification of a nonstandard N-glycosylation site in H_{5804P} and generation of recombinant viruses bearing N-glycan-deficient H proteins. (A) Schematic drawing of H_{5ko} and the four remaining N-glycosylation sites located in the ectodomain, and H_{7ko}, H_{9ko}, and H_{6ko}, indicating which potential N-glycosylation site is present in each protein. The site at position 152 is marked with an asterisk to indicate that it is the nonstandard type N-X-C. (B) Western blot comparing N-glycan-deficient H proteins to H_{5804P}. Note that H_{9ko} and H_{6ko} comigrate with the lower-molecular-weight bands of H_{5ko} and H_{7ko}. The proteins were expressed by transfection of expression plasmids in Vero dogsSLAMtag cells. (C) Cell surface biotinylation of N-glycan-deficient H proteins. Cells transfected with expression plasmids for H_{5804P}, H_{5ko}, H_{7ko}, or H_{6ko} were labeled with Sulfo-NHS-LC-biotin, immunoprecipitated with an antiserum recognizing the H protein cytoplasmic tail, and detected with a streptavidin-HRP conjugate. Western blots of cell lysates from the same experiment were used to quantify total H protein expression. Average relative surface expression is shown, and the blots are representative of three independent replicates. (D) Cell-cell fusion observed for wild-type and mutant H proteins. Confluent monolayers of Vero dogSLAMtag cells were transfected with F_{5804P} in combination with H_{5804P}, H_{5ko}, H_{7ko}, or H_{6ko} expression plasmid. The images were taken 24 h posttransfection at ×100 magnification. (E and F) Growth kinetics of the 5804PeH virus and the recombinant viruses expressing H_{5ko} or H_{6ko} in Vero dogSLAMtag cells shown as either cell-associated (E) or released (F) virus. The cells were infected at an MOI of 0.01, and samples were harvested daily for 5 days. Titers are expressed as $TCID_{50}$/ml, and the error bars indicate standard deviations.

four potential N-glycosylation sites, not all of which are used (17, 27, 31, 39). To clarify the role of N-glycans in the morbillivirus life cycle, we performed a comprehensive mutational analysis of CDV H protein N glycosylation and assessed its importance for virulence. We showed that five of the seven standard N-glycosylation sites in the ectodomain of the 5804P wild-type strain H protein are used and that an additional nonstandard site of the type N-X-C is used when few other sites are present. The H_{5804P} protein tolerates the deletion of all N-glycosylation sites without losing function, which has not been observed for any other paramyxovirus glycoproteins. However, viruses bearing N-glycan-deficient H proteins are completely attenuated *in vivo*.

CDV H protein processing and function are N-glycan independent. The morbillivirus H protein disulfide bonds generally join sites that are adjacent in the primary sequence (22) and thus may not need N-glycans for correct folding, in contrast to

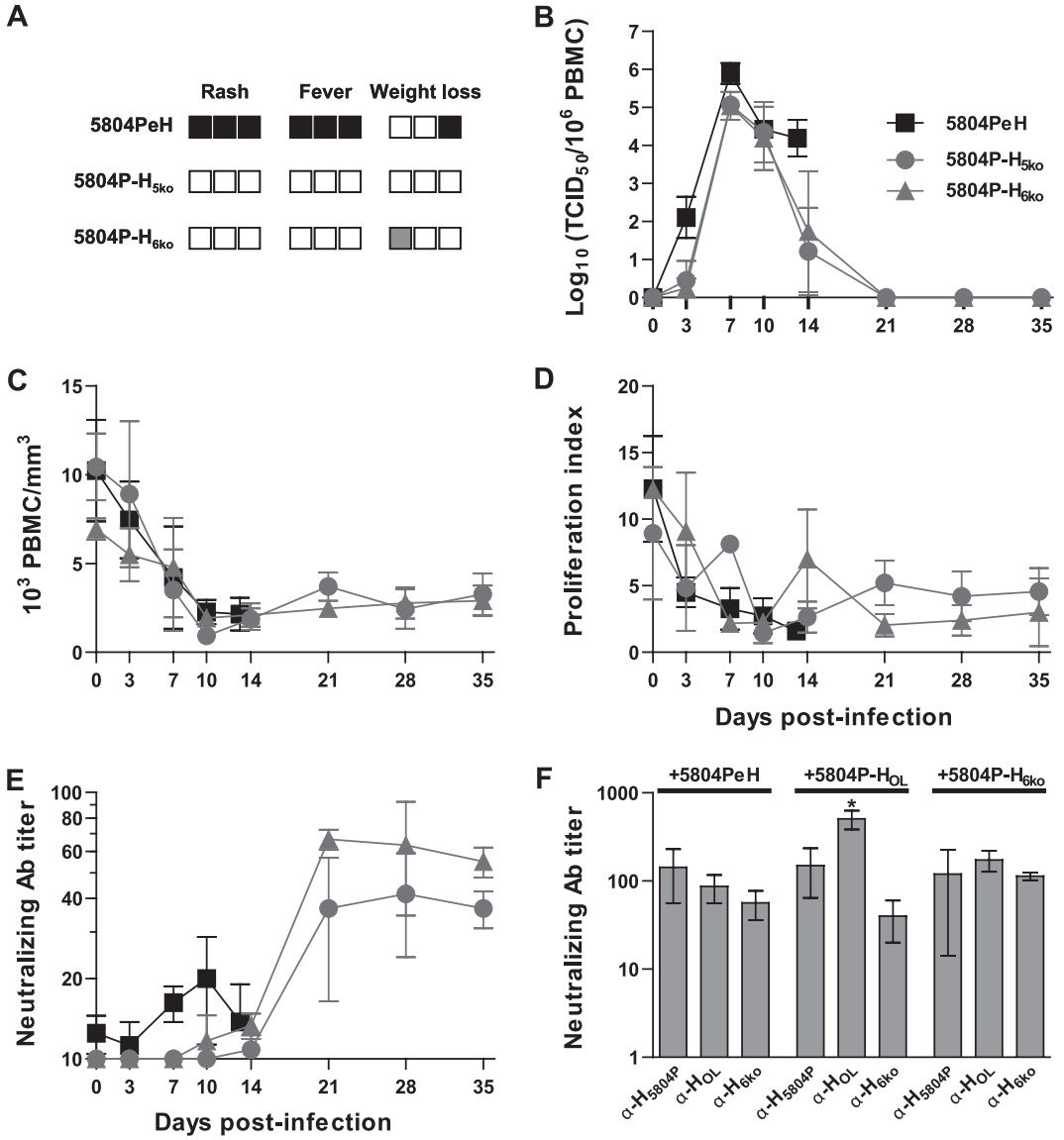

FIG. 5. Virulence of N-glycan-deficient viruses in ferrets. Groups of three or four animals were infected intranasally with 10^5 $TCID_{50}$ of either recombinant virus 5804P-H_{5ko} or 5804P-H_{6ko}. The results from the 5804PeH infections obtained in Fig. 2 are shown for comparison. (A) Virulence index. Each box represents one animal, and black represents the highest (2), gray an intermediate (1), and white the lowest (0) score, as detailed in Materials and Methods. (B) The course of cell-associated viremia is shown as the $\log_{10}$ of the virus titer per 10^6 PBMCs. (C) Total leukocyte counts, shown as 10^3 leukocytes per mm^3. (D) *In vitro* proliferation activities of lymphocytes over the course of disease. (E) CDV neutralizing-antibody response in plasma samples. Antibody titers are shown as reciprocals of the highest dilution in which CPE was observed. Days postinfection are indicated on the *x* axes, and the error bars represent standard deviations. (F) Cross-neutralization of recombinant viruses. Plasma from animals infected with 5804PeH, 5804P-H_{OL}, and 5804P-H_{6ko} were tested for efficiency of neutralization against the respective viruses. Neutralizing-antibody titers are shown as reciprocals of the highest dilution at which CPE was observed. The asterisk indicates statistical significance for 5804P-H_{OL} neutralization with α-H_{OL} serum ($P < 0.01$) compared to neutralization with α-H_{5804P} and α-H_{6ko} sera, and the error bars represent standard deviations.

the influenza virus hemagglutinin protein, which requires N-glycans to direct the formation of disulfide bonds between widely separated sites (12). Unlike fusion or other multifunctional proteins, where N-glycans play an important role in activation (2, 8, 16, 26, 30, 40, 47), the paramyxovirus attachment protein does not require cleavage to be functional. Despite this, sialic acid-binding attachment proteins are more sensitive to N-glycan deletion than CDV H (27, 31, 39), suggesting that their N-glycans may be involved in receptor recognition and attachment, while N glycosylation has not been demonstrated to play a role in morbillivirus interaction with its protein receptors SLAM and CD46 (4, 7, 18, 25, 46, 49). The observation that a completely deglycosylated H protein remains functional thus indicates a correlation between the N-glycosylation requirement and the folding and processing complexity of glycoproteins. While the ratio of cell surface to total cellular expression for N-glycan-deficient H proteins was not dramatically altered, their overall expression levels were re-

duced, demonstrating that N-glycans enhance H protein folding and transport and are added to the protein if sites are available, including nonstandard sites.

Was there a loss of N glycosylation during vaccine attenuation? The morbillivirus vaccine strains currently in use were produced decades ago by serial passage through various cell lines and eggs (11, 35). Unfortunately, the original seed viruses used in these passages are no longer available, so it is difficult to determine the exact changes that were accumulated during attenuation. The H proteins of wild-type CDV strains, such as 5804P, Snyder Hill, and A75/17, share six N-glycosylation sites (9). In addition, the 5804P H protein and other recent isolates have a site at N309 (14), and some Asian strains have acquired an eighth site at N584 (19, 29), both of which are not used. This demonstrates that wild-type H proteins have maintained the minimal complement of N-glycans needed to cause disease and ensure transmission and suggests that the Onderstepoort vaccine strain may have lost several N-glycosylation sites during the attenuation process. Our comparative neutralization assays demonstrated that not only are fully glycosylated and deglycosylated wild-type viruses neutralized with equal efficiency by all sera, including those raised against the vaccine H protein, but the vaccine H protein is more immunogenic than circulating wild-type H proteins. These results, together with the remarkable conservation of the wild-type N-glycosylation pattern despite high vaccine coverage, thus argues against a glycan shield escape mechanism in morbilliviruses, as has been proposed for HIV (20, 34, 53).

Reduced glycosylation alone does not explain vaccine strain attenuation. In our animal studies, introduction of the vaccine strain H protein into a wild-type virus resulted in complete attenuation, whereas the wild-type H protein with the vaccine strain N-glycosylation pattern remained lethal but with prolonged disease. In addition, all nonlethal viruses carrying 5804P H proteins resulted in prolonged inhibition of lymphocyte proliferation, while the virus with the vaccine H protein only transiently interfered with this activity. Our findings confirm previous reports that MeV wild-type H proteins are more immunosuppressive than vaccine H proteins (33), while complex N glycosylation was not required (54). This demonstrates the importance of H for vaccine attenuation and highlights the relative contributions of N glycosylation and primary sequence differences between vaccine and wild-type strain H proteins to virulence.

Since the SLAM-interacting residues are highly conserved among all strains, it is likely that the efficiency of H-F interactions, rather than receptor affinity, is another attenuating factor. However, the H protein residues 110 to 114, which are likely to be in close proximity to the F protein in the F-H complex (23), are conserved in all CDV strains. Thus, the attenuation observed for 5804P-H_{OL} may be due in part to the reduced ability of the wild-type F protein to efficiently interact with heterologous H proteins (23). In addition, any of the 60 amino acid differences between the vaccine and wild-type strains may result in conformational changes, thereby subtly altering protein function. While the N-glycan-deficient H proteins are otherwise identical to H_{5804P}, the lack of the N-glycan at N149 may also play a role in altering the interaction between F and H. This N-glycan is likely to be in close proximity to F (23), and its absence may destabilize the F-H complex. The virus bearing the vaccine H protein had a strongly reduced capacity to inhibit lymphocyte proliferation compared to the N-glycan-deficient viruses, which suggests that differences in contact inhibition are contributing factors (38, 54, 55).

ACKNOWLEDGMENTS

We thank all laboratory members for continuing support and lively discussions and Christoph Springfeld and Roberto Cattaneo for comments on the manuscript. We are particularly grateful to Nicholas Svitek and Stéphane Pillet for help with the animal studies.

This work was supported by grants from CIHR (MOP-66989), NSERC (299385-04), and CFI (9488) to V.V.M.

REFERENCES

1. **Anderson, D. E., and V. von Messling.** 2008. The region between the canine distemper virus M and F genes modulates virulence by controlling fusion protein expression. J. Virol. **82:**10510–10518.
2. **Bagai, S., and R. A. Lamb.** 1995. Individual roles of N-linked oligosaccharide chains in intracellular transport of the paramyxovirus SV5 fusion protein. Virology **209:**250–256.
3. **Baron, M. D.** 2005. Wild-type *Rinderpest virus* uses SLAM (CD150) as its receptor. J. Gen. Virol. **86:**1753–1757.
4. **Bartz, R., U. Brinckmann, L. M. Dunster, B. Rima, V. ter Meulen, and J. Schneider-Schaulies.** 1996. Mapping amino acids of measles virus hemagglutinin responsible for receptor (CD46) downregulation. Virology **224:**334–337.
5. **Bause, E., and G. Legler.** 1981. The role of the hydroxy amino acid in the triplet sequence Asn-Xaa-Thr(Ser) for the *N*-glycosylation step during glycoprotein biosynthesis. Biochem. J. **195:**639–644.
6. **Bonami, F., P. A. Rudd, and V. von Messling.** 2007. Disease duration determines canine distemper virus neurovirulence. J. Virol. **81:**12066–12070.
7. **Buchholz, C. J., D. Koller, P. Devaux, C. Mumenthaler, J. Schneider-Schaulies, W. Braun, D. Gerlier, and R. Cattaneo.** 1997. Mapping of the primary binding site of measles virus to its receptor CD46. J. Biol. Chem. **272:**22072–22079.
8. **Carter, J. R., C. T. Pager, S. D. Fowler, and R. E. Dutch.** 2005. Role of N-linked glycosylation of the Hendra virus fusion protein. J. Virol. **79:**7922–7925.
9. **Cherpillod, P., K. Beck, A. Zurbriggen, and R. Wittek.** 1999. Sequence analysis and expression of the attachment and fusion proteins of canine distemper virus wild-type strain A75/17. J. Virol. **73:**2263–2269.
10. **Cocks, B. G., C. C. J. Chang, J. M. Carballido, H. Yssel, J. E. de Vries, and G. Aversa.** 1995. A novel receptor involved in T-cell activation. Nature **376:**260–263.
11. **Confer, A. W., D. E. Kahn, A. Koestner, and S. Krakowka.** 1975. Biological properties of a canine distemper virus isolate associated with demyelinating encephalomyelitis. Infect. Immun. **11:**835–844.
12. **Daniels, R., B. Kurowski, A. E. Johnson, and D. N. Hebert.** 2003. N-linked glycans direct the cotranslational folding pathway of *Influenza virus* hemagglutinin. Mol. Cell **11:**79–90.
13. **Griffin, D. E.** 2006. Measles virus, p. 1551–1586. *In* D. M. Knipe, P. M. Howley, D. E. Griffin, R. A. Lamb, M. A. Martin, B. Roizman, and S. E. Straus (ed.), Fields virology, 5th ed. Lippincott Williams & Wilkins, Philadelphia, PA.
14. **Haas, L., W. Martens, I. Greiser-Wilke, L. Mamaev, T. Butina, D. Maack, and T. Barrett.** 1997. Analysis of the haemagglutinin gene of current wild-type canine distemper virus isolates from Germany. Virus Res. **48:**165–171.
15. **Hsu, E. C., C. Iorio, F. Sarangi, A. A. Khine, and C. D. Richardson.** 2001. CDw150(SLAM) is a receptor for a lymphotropic strain of measles virus and may account for the immunosuppressive properties of this virus. Virology **279:**9–21.
16. **Hu, A., T. Cathomen, R. Cattaneo, and E. Norrby.** 1995. Influence of *N*-linked oligosaccharide chains on the processing, cell surface expression and function of the measles virus fusion protein. J. Gen. Virol. **76:**705–710.
17. **Hu, A., R. Cattaneo, S. Schwartz, and E. Norrby.** 1994. Role of *N*-linked oligosaccharide chains in the processing and antigenicity of measles virus haemagglutinin protein. J. Gen. Virol. **75:**1043–1052.
18. **Hu, C., P. Zhang, X. Liu, Y. Qi, T. Zou, and Q. Xu.** 2004. Characterization of a region involved in binding of measles virus H protein and its receptor SLAM (CD150). Biochem. Biophys. Res. Commun. **316:**698–704.
19. **Iwatsuki, K., N. Miyashita, E. Yoshida, T. Gemma, Y.-S. Shin, T. Mori, N. Hirayama, C. Kai, and T. Mikami.** 1997. Molecular and phylogenetic analyses of the haemagglutinin (H) proteins of field isolates of canine distemper virus from naturally infected dogs. J. Gen. Virol. **78:**373–380.
20. **Johnson, W. E., H. Sanford, L. Schwall, D. R. Burton, P. W. H. I. Parren, J. E. Robinson, and R. C. Desrosiers.** 2003. Assorted mutations in the envelope gene of simian immunodeficiency virus lead to loss of neutralization resistance against antibodies representing a broad spectrum of specificities. J. Virol. **77:**9993–10003.

21. **Kumada, A., K. Komase, and T. Nakayama.** 2004. Recombinant measles AIK-C strain expressing current wild-type hemagglutinin protein. Vaccine **22:**309–316.
22. **Langedijk, J. P. M., F. J. Daus, and J. T. van Oirschot.** 1997. Sequence and structure alignment of *Paramyxoviridae* attachment proteins and discovery of enzymatic activity for a morbillivirus hemagglutinin. J. Virol. **71:**6155–6167.
23. **Lee, J. K., A. Prussia, T. Paal, L. K. White, J. P. Snyder, and R. K. Plemper.** 2008. Functional interaction between paramyxovirus fusion and attachment proteins. J. Biol. Chem. **283:**16561–16572.
24. **Martin, A., P. Staeheli, and U. Schneider.** 2006. RNA polymerase II-controlled expression of antigenomic RNA enhances the rescue efficacies of two different members of the *Mononegavirales* independently of the site of viral genome replication. J. Virol. **80:**5708–5715.
25. **Massé, N., M. Ainouze, B. Néel, T. F. Wild, R. Buckland, and J. P. M. Langedijk.** 2004. Measles virus (MV) hemagglutinin: evidence that attachment sites for MV receptors SLAM and CD46 overlap on the globular head. J. Virol. **78:**9051–9063.
26. **McGinnes, L., T. Sergel, J. Reittner, and T. Morrison.** 2001. Carbohydrate modifications of the NDV fusion protein heptad repeat domains influence maturation and fusion activity. Virology **283:**332–342.
27. **McGinnes, L. W., and T. G. Morrison.** 1995. The role of individual oligosaccharide chains in the activities of the HN glycoprotein of Newcastle disease virus. Virology **212:**398–410.
28. **Miletich, J. P., and G. J. Broze, Jr.** 1990. β Protein C is not glycosylated at asparagine 329. The rate of translation may influence the frequency of usage at asparagine-*X*-cysteine sites. J. Biol. Chem. **265:**11397–11404.
29. **Mochizuki, M., M. Hashimoto, S. Hagiwara, Y. Yoshida, and S, Ishiguro.** 1999. Genotypes of canine distemper virus determined by analysis of the hemagglutinin genes of recent isolates from dogs in Japan. J. Clin. Microbiol. **37:**2936–2942.
30. **Moll, M., A. Kaufmann, and A. Maisner.** 2004. Influence of N-glycans on processing and biological activity of the Nipah virus fusion protein. J. Virol. **78:**7274–7278.
31. **Ng, D. T. W., S. W. Hiebert, and R. A. Lamb.** 1990. Different roles of individual N-linked oligosaccharide chains in folding, assembly, and transport of the simian virus 5 hemagglutinin-neuraminidase. Mol. Cell. Biol. **10:**1989–2001.
32. **Oostra, M., E. G. te Lintelo, M. Deijs, M. H. Verheije, P. J. M. Rottier, and C. A. M. de Haan.** 2007. Localization and membrane topology of coronavirus nonstructural protein 4: involvement of the early secretory pathway in replication. J. Virol. **81:**12323–12336.
33. **Pfeuffer, J., K. Puschel, V. ter Meulen, J. Schneider-Schaulies, and S. Niewiesk.** 2003. Extent of measles virus spread and immune suppression differentiates between wild-type and vaccine strains in the cotton rat model (*Sigmodon hispidus*). J. Virol. **77:**150–158.
34. **Reitter, J. N., R. E. Means, and R. C. Desrosiers.** 1998. A role for carbohydrates in immune evasion in AIDS. Nat. Med. **4:**679–684.
35. **Rota, J. S., Z.-D. Wang, P. A. Rota, and W. J. Bellini.** 1994. Comparison of sequences of the H, F, and N coding genes of measles virus vaccine strains. Virus Res. **31:**317–330.
36. **Rouxel, R. N., N. Svitek, and V. von Messling.** 2009. A chimeric measles virus with canine distemper envelope protects ferrets from lethal distemper challenge. Vaccine **27:**4961–4966.
37. **Sawatsky, B., A. Grolla, N. Kuzenko, H. Weingartl, and M. Czub.** 2007. Inhibition of henipavirus infection by Nipah virus attachment glycoprotein occurs without cell surface down-regulation of ephrin-B2 or ephrin-B3. J. Gen. Virol. **88:**582–591.
38. **Schlender, J., J.-J. Schnorr, P. Spielhofer, T. Cathomen, R. Cattaneo, M. A. Billeter, V. ter Meulen, and S. Schneider-Schaulies.** 1996. Interaction of measles virus glycoproteins with the surface of uninfected peripheral blood lymphocytes induces immunosuppression *in vitro*. Proc. Natl. Acad. Sci. U. S. A. **93:**13194–13199.
39. **Segawa, H., A. Inakawa, T. Yamashita, and H. Taira.** 2003. Functional analysis of individual oligosaccharide chains of Sendai virus hemagglutinin-neuraminidase protein. Biosci. Biotechnol. Biochem. **67:**592–598.
40. **Segawa, H., T. Yamashita, M. Kawakita, and H. Taira.** 2000. Functional analysis of the individual oligosaccharide chains of Sendai virus fusion protein. J. Biochem. **128:**65–72.
41. **Stenflo, J., and P. Fernlund.** 1982. Amino acid sequence of the heavy chain of bovine protein C. J. Biol. Chem. **257:**12180–12190.
42. **Tatsuo, H., N. Ono, K. Tanaka, and Y. Yanagi.** 2000. SLAM (CDw150) is a cellular receptor for measles virus. Nature **406:**893–897.
43. **Taylor, M. E., and K. Drickamer.** 2006. Introduction to glycobiology, 2nd ed. Oxford University Press, Oxford, United Kingdom.
44. **Titani, K., S. Kumar, K. Takio, L. H. Ericsson, R. D. Wade, K. Ashida, K. A. Walsh, M. W. Chopek, J. E. Sadler, and K. Fujikawa.** 1986. Amino acid sequence of human von Willebrand factor. Biochemistry **25:**3171–3184.
45. **Vance, B. A., W. Wu, R. K. Ribaudo, D. M. Segal, and K. P. Kearse.** 1997. Multiple dimeric forms of human CD69 result from differential addition of *N*-glycans to typical (Asn-X-Ser/Thr) and atypical (Asn-X-Cys) glycosylation motifs. J. Biol. Chem. **272:**23117–23122.
46. **Vongpunsawad, S., N. Oezgun, W. Braun, and R. Cattaneo.** 2004. Selectively receptor-blind measles viruses: identification of residues necessary for SLAM- or CD46-induced fusion and their localization on a new hemagglutinin structural model. J. Virol. **78:**302–313.
47. **von Messling, V., and R. Cattaneo.** 2003. N-linked glycans with similar location in the fusion protein head modulate paramyxovirus fusion. J. Virol. **77:**10202–10212.
48. **von Messling, V., D. Milosevic, and R. Cattaneo.** 2004. Tropism illuminated: lymphocyte-based pathways blazed by lethal morbillivirus through the host immune system. Proc. Natl. Acad. Sci. U. S. A. **101:**14216–14221.
49. **von Messling, V., N. Oezguen, Q. Zheng, S. Vongpunsawad, W. Braun, and R. Cattaneo.** 2005. Nearby clusters of hemagglutinin residues sustain SLAM-dependent canine distemper virus entry in peripheral blood mononuclear cells. J. Virol. **79:**5857–5862.
50. **von Messling, V., C. Springfeld, P. Devaux, and R. Cattaneo.** 2003. A ferret model of canine distemper virus virulence and immunosuppression. J. Virol. **77:**12579–12591.
51. **von Messling, V., N. Svitek, and R. Cattaneo.** 2006. Receptor (SLAM [CD150]) recognition and the V protein sustain swift lymphocyte-based invasion of mucosal tissue and lymphatic organs by a morbillivirus. J. Virol. **80:**6084–6092.
52. **von Messling, V., G. Zimmer, G. Herrler, L. Haas, and R. Cattaneo.** 2001. The hemagglutinin of canine distemper virus determines tropism and cytopathogenicity. J. Virol. **75:**6418–6427.
53. **Wei, X., J. M. Decker, S. Wang, H. Hui, J. C. Kappes, X. Wu, J. F. Salazar-Gonzalez, M. G. Salazar, J. M. Kilby, M. S. Saag, N. L. Komarova, M. A. Nowak, B. H. Hahn, P. D. Kwong, and G. M. Shaw.** 2003. Antibody neutralization and escape by HIV-1. Nature **422:**307–312.
54. **Weidmann, A., C. Fischer, S. Ohgimoto, C. Rüth, V. ter Meulen, and S. Schneider-Schaulies.** 2000. Measles virus-induced immunosuppression in vitro is independent of complex glycosylation of viral glycoproteins and of hemifusion. J. Virol. **74:**7548–7553.
55. **Weidmann, A., A. Maisner, W. Garten, M. Seufert, V. ter Meulen, and S. Schneider-Schaulies.** 2000. Proteolytic cleavage of the fusion protein but not membrane fusion is required for measles virus-induced immunosuppression in vitro. J. Virol. **74:**1985–1993.